Targeted histone demethylation improves somatic cell reprogramming into cloned blastocysts but not postimplantation bovine concepti

Authors: Fanli Meng[1], Kathrin Stamms[1,2], Romina Bennewitz[1,3], Andria Green[1], Fleur Oback[1], Pavla Turner[1], Jingwei Wei[1,4] and Björn Oback[1,3#]

Author affiliations:

[1]AgResearch Ruakura Research Centre, Hamilton, New Zealand

[2]Present address: Institute of Nutrition, University Jena, Jena, Germany.

[3]Present address: Institute of Neurology, University Hospital Frankfurt, Frankfurt, Germany.

[4]Animal Science Institute, Guangxi University, Nanning, P.R China

[5]School of Medical Sciences, University of Auckland, Auckland, New Zealand

Corresponding Author: Björn Oback

AgResearch Ruakura Research Centre, Hamilton, New Zealand

Tel +64 7 838 5542, Fax +64 7 838 5536

E-mail bjorn.oback@agresearch.co.nz

ABSTRACT

Correct reprogramming of epigenetic marks in the donor nuclei is a prerequisite for successful cloning by somatic cell transfer. In several mammalian species, repressive histone (H) lysine (K) trimethylation (me3) marks, in particular H3K9me3, form a major barrier to somatic cell reprogramming into pluripotency and totipotency. We engineered bovine embryonic fibroblasts (BEFs) for the doxycycline-inducible expression of a biologically active, truncated form of murine Kdm4b, a demethylase that removes histone 3 lysine 9 trimethylation (H3K9me3) and H3K36me3 marks. Upon inducing *Kdm4b*, H3K9me3 and H3K36me3 levels reduced ~3-fold and ~5-fold, respectively, compared to non-induced controls. Donor cell quiescence has been previously associated with reduced somatic trimethylation levels and increased cloning efficiency in cattle. Simultaneously inducing *Kdm4b* expression (via doxycycline) and quiescence (via serum starvation), further reduced global H3K9me3 and H3K36me3 levels by a total of 18-fold and 35-fold, respectively, compared to non-induced, non-starved control fibroblasts. Following somatic cell transfer, *Kdm4b*-BEFs reprogrammed significantly better into cloned blastocysts than non-induced donor cells. However, detrimethylated donors and sustained *Kdm4b*-induction during embryo culture did not increase rates of post-blastocyst development from implantation to survival into adulthood. In summary, overexpressing *Kdm4b* in donor cells only improved their reprogramming into early preimplantation stages, highlighting the need for alternative experimental approaches to reliably improve somatic cloning efficiency in cattle.

2

INTRODUCTION

Despite their morphological and functional diversity, different somatic cell types within an individual contain the same genetic information. Phenotypic differences are stabilised by epigenetic modifications, such as histone methylation, that regulate cell-specific gene activity. 'Reprogramming' of these epigenetic marks naturally occurs during mammalian gametogenesis and preimplantation embryogenesis [1]. Cloning by somatic cell transfer (SCT), can artificially reprogram somatic cells [2]. During SCT, a somatic donor cell is fused with an enucleated recipient oocyte (or cytoplast). Epigenetic marks on the donor chromatin are then reprogrammed by cytoplast factors that are still largely unknown. In some cases, the donor nucleus regains totipotency, i.e. the ability to form all embryonic and extra-embryonic lineages in a viable animal. However, totipotency reprogramming of somatic cells is inefficient due to a strong resistance to erase the epigenetic memory of previous lineage decisions and restart embryonic gene transcription [3]. This reprogramming resistance compromises development of the SCT embryo, resulting in aberrant methylation patterns of DNA [4] and histones [5] and dysregulation of gene expression [6].

To improve epigenetic reprograming after SCT, several approaches have been used with some success. First, in chronological order of discovery, pharmacological histone deacetylation inhibitors (HDACi) induce hyperacetylated, transcriptionally permissive chromatin and can increase *in vivo* cloning efficiency in mouse [7, 8] and pig [9] but their impact in cattle species remains controversial [10-12]. Second, cloned mouse embryos often overexpress *Xist*, a noncoding gene responsible for X chromosome inactivation, from the active X chromosome, ectopically downregulating many X-linked genes necessary for embryonic development [13]. Normalizing *Xist* expression by gene knockout or knockdown can increase cloning efficiency by up to 20% per embryo transferred [13, 14]. Third, we discovered that heterochromatic H3K9me3 marks pose a major epigenetic barrier in mouse cloning, antagonizing an open, transcriptionally permissive

3

chromatin configuration [15]. Overexpressing the histone lysine demethylase *Kdm4b* in donor cells decreased H3K9me3 levels in embryonic stem cells [15] and this demethylation was even more pronounced in mouse embryonic fibroblasts (MEFs) [16]. Reduced H3K9me3 donor levels correlated with improved development of embryos cloned from ESCs [15] and, even more markedly, from MEFs [16]. The principle we first described in mouse was confirmed by other groups, using various *Kdm4* isoforms, and extended to other mammalian species. In mouse, *Kdm4b* expression was aberrant in developmentally arrested SCT 2-cells, a defect which could be overcome by injecting exogenous *Kdm4b* mRNA into enucleated MII oocytes prior to SCT [17]. Injecting SCT embryos with *Kdm4d* mRNA also markedly increased clone development in mouse [18]. The latter approach was then used for overexpressing another related H3K9me3 demethylase, *KDM4A*, to improve blastocyst formation rate in human SCT embryos [19]. In non-human primates, successful cloning of cynomolgus monkeys was also attributed to *KDM4D* mRNA injection [20]. Combined with HDACi treatment, this approach greatly improved blastocyst development and pregnancy rate of transplanted SCT embryos [20]. Overexpressing *KDM4D* or *KDM4E* via mRNA injection into bovine SCT 1-cell reconstructs also increased embryo development into high-quality blastocysts and survival into viable calves [21]. In pig, KDM4A mRNA injection improved *in vitro* but not in *in vivo* development [22]. In sheep, donor cell pretreatment with recombinant KDM4D protein improved *in vitro* development of SCT embryos [23] but *in vivo* development was not reported. A practical advantage of these mRNA- or protein-based approaches is that they are non-transgenic, which increases their applicability for agriculture.

Fourth, cellular quiescence by serum starvation ("G_0") has recently been shown to induce globally reduced DNA and histone trimethylation that correlate with a more relaxed G_0 chromatin state and elevated somatic cell reprogrammability after SCT [24]. Specifically, H3K9me3 hypomethylation persisted in SCT-derived embryos and correlated with their increased survival into cloned cattle.

4

Collectively, these findings established H3K9me3 as a major epigenetic barrier that obstructs restoration of totipotency following SCT.

Here we focused on the functional consequences of overexpressing murine *Kdm4b* in bovine embryonic fibroblasts (BEFs). We show a strong decrease in somatic H3K9me3 and H3K36me3 (H3K9/36me3) levels, which was rapidly restored in reconstructed bovine embryos after SCT. Sustained *Kdm4b* expression moderately increased reprogramming into cloned blastocysts. However, this treatment did not improve *in vivo* survival of cloned blastocysts into viable calves, indicating the need for alternative experimental strategies to robustly elevate cloning efficiency in livestock.

5

MATERIALS AND METHODS

All animal studies were undertaken in compliance with the New Zealand Animal Welfare Act and were approved by the Ruakura Animal Ethics Committee.

Vector construction

To generate the doxycycline (Dox)-inducible *Kdm4b-Egfp* piggybac (pB) transposon vectors, a pBS31 flp-in vector, kindly provided by J. Antony [15], was digested with *NotI* and *SalI* to excise the ~2 kb *Kdm4b-Egfp* insert. This fragment comprises the 1-424 amino acid fully functional murine *Kdm4b*, fused to an N-terminal *Egfp* [25]. PB-TET-MKOS, a gift from Andras Nagy (Addgene plasmid # 20959), was modified to replace the original Tet-ON promoter [26] with a synthetic (GeneArt, Thermo Fisher, NZ) Dox-inducible P_{TRE3G} promoter that provides very low basal expression and high maximal expression after induction [27]. This pB-TRE3G response vector was further modified by replacing the *βgeo* cassette with a *puromycin* selection marker, co-expressed with *Kdm4b-Egfp* via an internal ribosome entry site (IRES). Following *NotI*/*SalI* digest and cohesive end ligation, the newly generated *pB-TRE3G_Kdm4b-Egfp* vector was isolated using a PureLink™ HiPure Plasmid Filter Kit (Thermo Fisher, New Zealand) and validated by restriction enzyme digestion and sequencing analysis.

Generation of stable BEF strains for inducible expression of *Kdm4b-Egfp*

As parental cells, a rejuvenated Dox-inducible driver line, based on BEFs carrying the Tet-On 3G transactivator driven by a human elongation factor 1 alpha (EF1α) promoter (Clonetech, Cat. No. 631167) was used (Green and Oback, manuscript in preparation) and induced with 2 µg/ml Dox (Sigma) two hours prior to transfection. At 70-80% confluence, these neomycin-resistant cells ('BEF5-Tet') were co-transfected with 2.5 µg *pB-TRE3G_Kdm4b-Egfp* using lipofection

6

(Lipofectamine^{TM} LTX/PLUS^{TM}, Thermo Fisher) and 2.5 µg pB transposase *CAGG-PBase*

(pCyL43) [28]. Following selection with 1 µg/µl puromycin for seven days, 24 resistant cell clones

were picked with cloning rings, subcloned onto gelatine-coated plates, expanded in puromycin-free

medium, cryopreserved and two clones analyzed for Dox-inducible *Kdm4b-Egfp* expression.

Induction of transgene expression

Both *Kdm4b-Egfp* clones were cultured as described [29] in the presence of 2 µg/ml Dox for 24

hours. Induced cells were analyzed for EGFP fluorescence on a FACSCalibur™ (Becton and

Dickinson, USA). To assess reversibility of *Kdm4b-Egfp* expression, induced BEFs were washed,

re-seeded in Dox-free medium and analyzed for EGFP fluorescence one day later. For analyses of

serum-starved cells, fresh DOX was added to the low-serum cell culture medium every 2 days,

while non-starved cells were induced for 2 days to prevent them from becoming confluent (Figs. 2-

4, Tables 1-3). For inducing *Kdm4b* expression in embryos, SCT reconstructs were handled in

media without Dox until the end of chemical activation, when they were placed into single drops

with fresh culture medium ± Dox on D0, D3 and D5.

RNA Extraction and PCR

Cells were lysed in 50 µL *RNA*GEM™ Tissue *PLUS* (containing 1.0 µL *RNA*GEM™) and cDNA

synthesized as described [30]. Reverse transcriptase was omitted in one sample each time a batch

was processed for cDNA synthesis ('-RT'). Primers were designed using NCBI/ Primer-BLAST

and synthesized by Integrated DNA Technologies (IDT, IA, USA). For quantitative RT-qPCR

(qPCR), a LightCycler (Roche) was used with primers against transgene-derived *Kdm4b* (forward:

5'- AGAAGACACCGGGACCGATC-3', reverse: 5'- TGAATTCATCCATGGTGGGG-3', 190 bp

amplicon), *ZFP37* (forward: 5'-CCTCAATGGGGTATCAGGCTC-3', reverse: 5'-

7

GATGGACTTCTTTTCCATTGGCT-3', 156 bp amplicon) and *18S* (forward: 5'-
AACGTCTGCCCTATCAACT-3', reverse: 5'-AACCTCCGACTTTCGTTCT-3', 70 bp amplicon).

All the reactions were performed with the KAPA SYBR® FAST qPCR Kit (Kapa Biosystems, MA,
USA), which consisted of 0.4 µl of each primer (10 µM), 5.0 µl master mix, 2.2 µl DEPC water and
1.0-2.0 µl cDNA template. The following four-segment program was used: 1) denaturation (10 min
at 95°C), 2) amplification and quantification (20 sec at 95°C, 20 sec at 55°C–60°C, followed by 20
sec at 72°C with a single fluorescent measurement repeated 45 times), 3) melting curve (95°C, then
cooling to 65°C for 20 sec, followed by heating at 0.2°C/sec to 95°C while continuously measuring
the fluorescence), and 4) cooling to 4°C. cDNA from bovine brain tissue provided a positive
control. Product identity was confirmed by gel electrophoresis and melting curve analysis. For
relative quantification, external standard curves were generated from serial 10-log dilutions for each
gene in duplicate or triplicate. One high-efficiency curve ($3.6 \geq$ slope ≥ 3.1, $R^2 > 0.99$) was saved
and imported for relative quantification compared to 18S RNA as described [30]. A 'no template'
control reaction was included in every run for each primer pair to test for DNA contamination and
formation of primer–dimers.

Quantitative Immunofluorescence (IF)

For each comparison, induced and non-induced cells were processed and analyzed in parallel. Cells
were fixed and permeabilized simultaneously in 3.6% (w/v) paraformaldehyde/1% (w/v) Triton X-
100 in PBS for 10 min, blocked with 2.5% (w/v) bovine serum albumin in PBS, all at room
temperature, and incubated overnight at 4-8°C with the primary antibody specific for H3K9me3 (for
IF: rabbit polyclonal, gift by T. Jenuwein and previously validated for bovine [24] or mouse
monoclonal, #c15200146, Diagenode; for western analysis: mouse monoclonal, #c15200146,

8

Diagenode), H3K36me3 (rabbit polyclonal, #9763, Cell Signaling or # c15410058, rabbit

polyclonal, Diagenode), H3K27me3 (mouse monoclonal, # c15200181, Diagenode) and anti-EGFP

(mouse monoclonal, # A-11120, Thermo Fisher) . The next day, cells were washed in PBS-0.05%

Tween 20 and incubated for 1 h at room temperature with Alexa Fluor® 488 or 568 donkey anti-

goat, -mouse, -rabbit or –sheep secondary IgG antibodies (Thermo Fisher). DNA was

counterstained with 5 µg/ml Hoechst 33342 (Sigma). Preparations were washed in PBS and H_2O

before mounting (DAKO, Med-Bio Ltd., New Zealand) onto glass slides. Wide-field

epifluorescence (Olympus BX50) images were captured in monochromatic mode with a digital

camera (Spot RT-KE slider) and Spot Basic software (v4.6).

SCT reconstructs were first fixed in 4% paraformaldehyde (30 min at 4^0C) and then permeabilized

in 0.1% Triton X-100 (5 min at room temperature) before blocking and immunostaining. Negative

controls were processed the same way with blocking buffer instead of primary antibodies.

Normalisation and quantification of global H3K9me3 levels was conducted on greyscale images in

ImageJ. The Hoechst-stained region of interest (ROI) around the nucleus was outlined. Mean grey

value intensity, measured at 3 random cytoplasmic locations, was subtracted from the mean ROI

intensity. This background-corrected mean intensity represents the sum of grey values of all pixels

in the ROI divided by the number of pixels and is referred to as normalized pixel intensity.

Following quantification, images were pseudo-colored in PowerPoint by using the Recolor

function.

Western blot

Histones were extracted using the EpiQuik^{TM} Total histone extraction kit (Epigentek, Cat- OP-0006-

100). Histone extracts (10-15 µg per lane) were separated on a 15% SDS PAGE gel, transferred

onto a nitrocellulose membrane and probed with primary antibodies specified above, with the

9

additional use of anti-H3K27me3 (rabbit polyclonal, #07-449, Millipore). Following incubation

with a secondary antibody conjugated with horseradish peroxide, the modified histones were

visualised with enhanced chemiluminescence. Signal intensity was normalized for three invariant

histone bands (Ponceau S stain) and quantified using Quantity One software (Bio-Rad Laboratories

Inc.).

Generating SCT embryos and calves

Cultured *Kdm4b*-BEFs were serum-starved in medium containing 0.5% FCS for 3-6 days and

harvested by trypsinization. Prior to each SCT run, cells were validated for successful induction

of *Kdm4b* by monitoring EGFP signal with a digital fluorescence microscope (AMG-EVOS,

Thermo Fisher). For IF analysis and embryo transfer (ET), zona-free SCT was performed as

described [31]. Briefly, *in vitro* matured (IVM) non-activated metaphase II (MII)-arrested

oocytes were derived from ovaries of slaughtered mature cows [31]. After IVM for 18-20 h, the

cumulus-corona was dispersed by vortexing in bovine testicular hyaluronidase. Oocytes with a

first polar body were chosen for enucleation. At 23-25 h post start of IVM, donor-cytoplast

couplets were automatically aligned and electrically fused at 2.0 kV/cm. Reconstructed SCT

embryos were artificially activated 3-4 h post-fusion, using a combination of ionomycin and 6-

dimethylaminopurine (6-DMAP). After 4 h in 6-DMAP, reconstructs were washed three times in

Hepes-buffered SOF (HSOF) and transferred into AgResearch-SOF single culture medium

droplets for sequential *in vitro* culture (IVC). Embryo cultures were overlaid with mineral oil

and kept in a humidified modular incubation chamber (ICN Biomedicals Inc., Aurora, OH)

gassed with 5% CO_2, 7% O_2, and 88% N_2. *In vitro* development was assessed on Day (D) 7 or

D8 after fusion and morphological grade 1-2 quality embryos were non-surgically transferred

singularly to synchronized recipient cows [31]. Fetal development was monitored by regular

ultrasonography and rectal palpation throughout gestation.

In vitro fertilised (IVF) embryos

IVM oocytes from slaughterhouse ovaries of mixed breed dairy cows were fertilized with

frozen–thawed semen from a sire with proven in vitro fertility as described [32]. For cumulus-

free cultures, the corona was dispersed after IVF for 22–24 h by vortexing oocytes in 500 µl of 1

mg/ml bovine testicular hyaluronidase in HSOF, followed by two washes in HSOF. For

sequential IVC, 10 embryos were pooled in 20 µl of AgResearch-SOF medium and cultured for

8 days (D0: fertilization) as described for SCT embryos.

Statistical analysis

Values are the average of several replicates ± SEM. For the quantification of fluorescent signals

and western blot bands, significance was determined by t-tests of normalized pixel intensities and

expression ratios, respectively. For comparing *in vitro* development, significance was determined

using the two-tailed Fisher exact test for independence in 2 X 2 tables. Significance was accepted

as P<0.05. Unless stated otherwise, "N" denotes the number of samples analysed; "n" denotes the

number of replicate experiments.

RESULTS

Rejuvenated bovine fibroblasts express Dox-inducible *Kdm4b*

11

To reduce H3K9/36me3 levels in bovine clones, we generated a piggyBac (PB) transposon vector for tetracycline-responsive (TRE3G) expression of a previously characterized murine *Kdm4b-EGFP* fusion construct [15], encompassing the fully functional catalytic KDM4B domain, translationally linked to a puromycin expression cassette (Fig. 1A). Using a two-step process of sequential rejuvenation (Fig. 1B), we first re-derived several BEFs carrying a constitutive *Tet-On 3G* transactivator construct (step 1), before transfecting these neomycin-resistant clonal cell strains ('BEF5-Tet') with *TRE3G_Kdm4b-Egfp* for a second round of rejuvenation (step 2). Detailed derivation and characterisation of selected BEF-Tet driver strains and inducible TRE-responder strains will be published elsewhere (Green and Oback, manuscript in preparation). To test induction of transgene expression, two rejuvenated *Kdm4b-Egfp* clonal BEF strains (#1, #2) were cultured in the presence of Dox for 24 hours. Due to the fusion with *Egfp*, cells expressing *Kdm4b* could be readily monitored and were analyzed by flow cytometry. An average 85% and 94% of *Kdm4b* strains #1 and #2, respectively, displayed EGFP fluorescence (Fig. 1C). We also examined the kinetics for switching off *Kdm4b-Egfp* expression. Within 24 hours after Dox removal, cells returned to a profile that was indistinguishable from non-induced cells, confirming that inducible transgene expression was fully reversible (Fig. 1C).

KDM4B and serum starvation specifically reduce H3K9me3 and H3K36me3 in BEFs

We next evaluated the enzymatic activity of transgene-encoded murine KDM4B in both clonal BEF strains. Pairwise sequence alignment of bovine (XP_024850763.1) vs mouse (NP_742144.1) KDM4B showed high sequence conservation, with overall 87.7% identity (amino acids 1-424) and 100% identity within the JMJC domain (amino acids 176-292). To determine the effect on histone methylation, induced and non-induced *Kdm4b-Egfp* BEFs were analysed for levels of H3K9me3, and H3K36me3, as well as H3K27me3, which should not be directly targeted, by

immunofluorescence and immunoblots. Induced cells expressing KDM4B-EGFP showed markedly reduced H3K9me3 and H3K36me levels (Fig. 2). In non-starved KDM4B-EGFP positive nuclei, signal intensity for H3K9me3 and H3K36me3 was 4-fold and 6-fold lower, respectively, than in non-induced controls (P<0.001), while non-targeted H3K27me3 control levels were not significantly changed (Fig. 2A, B). Following serum starvation and *Kdm4b* overexpression, signal intensity for H3K9me3 and H3K36me3 was 6-fold and 11-fold reduced, respectively, relative to non-induced controls (P<0.001), while H3K27me3 levels were again not significantly affected (Fig. 2A, B). Serum starvation has been shown to globally reduce trimethylation levels in bovine fibroblasts and increase their cloning efficiency [24]. We therefore analysed the effect of *Kdm4b* overexpression in non-starved vs serum-starved BEFs separately. Serum starvation alone reduced H3K9me3 levels 4-fold vs 8-fold (P<0.001) and H3K36me3 levels 3-fold vs 6-fold (P<0.001) in non-induced vs induced cells, respectively. Overall, Dox-induced, serum-starved *Kdm4b*-BEFs had the lowest H3K9me3 and H3K36me3 levels, 18-fold and 35-fold reduced, respectively, relative to non-induced, non-starved control BEFs.

To independently validate these results, we performed western blot analyses on bulk histones (Fig. 2C, D). For non-starved *Kdm4b*-BEFs, H3K9me3 and H3K36me3 levels dropped ~2-fold (P=0.05) and ~3-fold (P<0.05), respectively, compared to non-induced controls. Upon *Kdm4b* induction in serum-starved cells, H3K9me3 and H3K36me3 levels dropped ~4-fold (P<0.05) and ~6-fold (P<0.01), respectively, compared to non-induced controls. As for the IF characterization, Dox-induced, serum-starved *Kdm4b*-BEFs had the lowest H3K9me3 and H3K36me3 levels, while H3K27me3 levels were not significantly altered. For both induced and non-induced conditions, serum-starved BEFs showed lower normalized band intensities for all three histone trimethylations. Thus, both detection methods showed that BEFs were strongly and specifically de-trimethylated by serum starvation and inducible *Kdm4b*-overexpression.

13

Up-regulation of *Zfp37* gene expression in *Kdm4*-BEFs

We previously surveyed the global transcriptional impact of *Kdm4b*-mediated reduction in H3K9/36me3 levels in female *Kdm4b-Egfp* MEFs by microarray, mRNA-seq and qPCR [16]. Across all three assays, the only consistently and significantly changed candidate transcript with a direct linkage to heterochromatin was *Zfp37*, which encodes a heterochromatin-associated zinc finger protein expressed in brain and testis [33]. Using RT-qPCR, Dox-induced, serum-starved donor BEFs showed 37-fold higher *Kdm4b* levels, resulting in a 4-fold up-regulation (P<0.05) of *Zfp37* (Fig. 3).

Reduced H3K9me3 and H3K36me3 donor cell levels are rapidly restored after SCT

We then examined how reduced H3K9/36me3 levels in serum-starved *Kdm4b*-induced BEFs changed after SCT and subsequent *in vitro* embryo development in the absence of Dox. SCT reconstructs from induced and non-induced *Kdm4b*-BEFs were fixed at various time points after electrofusion and analyzed by immunofluorescence for the presence of the *Kdm4b-Egfp* transgene and H3K9/36me3. Ten minutes after fusing BEFs with the cytoplast, the EGFP signal was still visible within the SCT reconstruct but had mostly disappeared after 3 h and was no longer detectable 8 h and 24 h post SCT (Fig. S1A). Following Dox induction during IVC, *Kdm4b-Egfp* expression was re-initiated in most blastocysts (16/18=89%) but the proportion of positive cells within each blastocyst was variable and staining appeared more prominent in the inner cell mass (ICM) compared to the trophectoderm (TE) (Fig. S1B).

Immediately after fusion, reduced H3K9/36me3 signals were still observed in SCT reconstructs from induced compared to non-induced donors (Fig. 4A). However, 3 h post-fusion the differences had diminished in the newly formed pseudo-pronuclei and after 8 h SCT reconstructs derived from

14

induced and non-induced donor cells displayed similar H3K9me3 and H3K36me3 intensities, respectively (Fig. 4B). No further differences in H3K9/36me3 staining intensities were observed at the 2-cell (24 h) stage (Fig. 4B). Control IVF embryos were analysed in parallel at chronologically similar developmental stages, considering that fertilization takes place about five hours post-insemination (hpi). At 8 hpi, most zygotes contained separate maternal and paternal PN, with the latter being relatively hypotrimethylated (Fig. S2A). At the 2-cell stage, interphase chromatin in IVF vs SCT embryos, both induced and non-induced, showed no significant differences in H3K9/36me3 levels (Fig. S2B). This changed at the blastocyst stage, when non-induced SCT embryos were H3K9me3 hypermethylated in the ICM and TE, while induced SCT embryos did not differ significantly from IVF controls (Fig. S2C, D). Non-induced SCT embryos were also H3K36me3 hypermethylated in the ICM compared to induced embryos, but both SCT groups differed significantly from IVF embryos (Fig. S2C, D). Thus, reduced H3K9/36me3 levels in BEFs were initially restored in SCT embryos but hypotrimethylation could be re-induced in the ICM.

Sustained *Kdm4b* induction improves blastocyst development *in vitro*

To determine the effect of H3K9/36me3 hypomethylation on donor cell reprogrammability, we cultured SCT reconstructs to the blastocyst stage. Culture for embryos reconstructed with induced vs non-induced *Kdm4b*-BEFs was first performed without Dox, which showed no significant difference in total and high-quality blastocyst development (52 vs 50% and 32% vs. 28%, respectively, Table 1). We then continued induction during SCT embryo culture, refreshing Dox every two days, to determine the effect of continuous *Kdm4b* expression on development. Under these conditions, there was a significant improvement of total and high-quality blastocyst development (55% vs. 40%, P<0.0001 and 28% vs 21%, P<0.01, respectively, Table 2) compared to non-induced controls.

15

Reduced H3K9me3 and H3K36me3 donor cell levels do not improve fetal development *in vivo*

Long-term in utero development is a more stringent measure of donor cell reprogrammability into totipotency than blastocyst formation [34]. To assess the *in vivo* developmental potential of cloned embryos generated from *Kdm4b*-induced donor cells and embryos, which showed significantly improved blastocyst development compared to non-induced controls, D7 blastocysts were transferred into recipient cows. In three independent experiments, representing both *Kdm4b*-BEF strains, there were no significant differences for induced vs non-induced clones in establishing pregnancies and development to term (Table 3). One female calf, derived from non-induced *Kdm4b*-BEF donors, was delivered by Caesarean section on 18/01/2018. After two weeks, an ear biopsy was taken to re-derive ear skin fibroblasts. Cultured fibroblasts were Dox-treated for 48 hours, which induced KDM4B-EGFP signal in the re-derived cells (data not shown). Throughout gestation, we did not observe a difference in the frequency of hydroallantois, the most common complication with bovine SCT fetuses in our hands, which occurred twice in each treatment group ($2/12 = 17\%$ vs $2/13 = 15\%$ for non-induced vs induced pregnancies, respectively). Thus, the moderate 1.4-fold increase in blastocyst reprogramming did not translate into an equivalent increase in post-blastocyst development.

DISCUSSION

Here we show that the combination of *Kdm4b*-overexpression and serum starvation enhances simultaneous H3K9me3 and H3K36me3 removal from somatic donor cell chromatin. Following SCT, this hypomethylated epigenome reprograms better *in vitro* but not *in vivo*.

Effects of H3K9/36me3 erasure on donor cell and embryo transcriptome

16

The beneficial effect of H3K9me3 removal on epigenetic reprogramming during SCT is well described. A repressive modification, H3K9me3 causes heterochromatin formation [35] and epigenetic silencing [36]. Heterochromatinization generally marks megabase-scale gene-poor regions and repetitive elements, restricting access to chromatin-binding factors. Consequently, gene expression changes in Dox-induced somatic donor cells have been relatively minor [16]. Among the changed transcripts, the only direct linkage to heterochromatin was *Zfp37*. The encoded zinc finger protein is expressed in brain and testis, where it specifically associates with the heterochromatin adjoined to nucleoli [33]. Up-regulation of *Zfp37* was confirmed in *Kdm4b*-BEFs, supporting a conserved role of this target gene whose regulatory role is unknown. Overexpressing *Zfp37* in donor cells or embryos may shed light on its function and directly improve cloned blastocyst formation. However, similar attempts at rescuing development with *KDM4*-induced target genes, such as *Zscan4d* in mouse [18] and *SUPT4H1* in cattle [21], have failed. This highlights that a core gene regulatory network, rather than a single master regulatory transcription factor, may govern totipotency reprogramming.

In contrast to H3K9me3, it is presently unclear if and how reduced H3K36me3 levels affect reprogramming of the donor genome. H3K36me3 is present at the coding regions of transcribed genes [37]. Trimethylation of active H3K36 and repressive H3K27 is broadly mutually exclusive in euchromatin, which may prevent spreading and accumulation of silencing marks [37]. Indeed, global loss of H3K36me3 redistributes H3K27me2/3 from its endogenous sites to active gene bodies and mis-regulates gene expression [37]. Depleting H3K36me3 may have enriched for H3K27me3, for example, in regions maintaining X-linked gene expression and X chromosome inactivation in females [38]. These regions have been implicated in impairing SCT reprogramming through ectopic expression of *Xist* during the preimplantation period in both sexes, which can be corrected by removing or repressing *Xist* [13, 14, 22, 39].

17

In SCT embryos, exogenous expression of different KDM4 variants has normalized activation of developmentally regulated genes, including *Kdm4b* (but not *Kdm4d*) and *Kdm5b* in mouse [17], *KDM4A* in pig [22] and *KDM1B*, *KDM4C*, *KDM4D* and *KDM4E* in cattle [21]. Some of these normalized genes lie within 'reprogramming-resistant regions' that fail to activate correctly at embryonic genome activation (EGA) in SCT embryos. These relatively gene-poor regions are enriched for specific repeat sequences and conserved among different somatic cell types and species [18, 19]. Importantly, these regions are marked by H3K9me3 and enzymatic erasure of H3K9me3 facilitates their transcriptional activation, restoring the global transcriptome of SCT embryos [18, 19, 21, 22]. Activation of repeat sequences around EGA is important for preimplantation development [40, 41]. In *Kdm4b*-expressing MEFs, endogenous retrovirus repeats, as well as major satellites, and intact LINEs, were derepressed [16]. Likewise, overexpression of *Kdm4d* and *KDM4E* partially relieved repression of endogenous retrotransposons and satellite I sequences in mouse [18] and bovine [21] embryos, respectively, around EGA.

Serum starvation enhances H3K9/36me3 demethylation

We show that in serum-starved cells, histone trimethylation reduction for both H3K9me3 and H3K36me3 was about 2-fold greater under both non-induced and induced conditions. This 2-fold greater downregulation was observed using both IF and western blot analysis, even though the relative fold-changes were slightly different. It shows that serum starvation about doubles the effect of exogenously expressed *Kdm4b* on reducing histone trimethylation, confirming and extending previous results for H3K9me3 and H3K36me3 levels, respectively [24]. This additive effect of serum starvation suggests that it operates by a different molecular mechanism than induced *Kdm4b*. We previously reported that serum starvation about halves the amount of H3K9me3 in non-transgenic primary bovine cell types, resulting in a more relaxed chromatin structure and providing

18

a molecular correlate for the elevated reprogrammability of quiescent donor cells into totipotency. This halving may be due to starved cells acquiring non-methylated histones during S-phase but not re-instating trimethylation upon serum starvation, allowing completion of the last DNA replication and mitosis before entering a non-proliferative G_0 state [24].

Reduced H3K9/36me3 levels after SCT reprogramming

Globally reduced H3K9/36me3 levels in induced donor cells initially persisted in reconstructed embryos but returned to non-induced control levels within 3-8 hours after SCT, probably due to the high initial cytoplasmic dilution factor. This kinetics is similar to the restoration of H3K9/36me3 marks previously observed for MEFs [16]. Metaphase-arrested mouse cytoplasts can also restore H3K9 methylation in transplanted male pronuclei within three hours [42]. The rapid gain of methylation at H3K9 sites suggests enzymatic action rather than slow incorporation of already trimethylated histones into newly synthesized DNA. At the 2-cell stage, we found no significant differences in histone trimethylation levels between SCT embryos derived from normal vs hypomethylated BEF donors and IVF controls. Following continuous Dox-induction during culture, we observed reactivation of the transgene mostly restricted to the ICM. This may be due to the behavior of exogenous promoters, which reveals a large degree of variation depending on the cell type, vector design, orientation and integration site [43]. During differentiation, promoter activities of constitutive promoters generally decrease, suggesting the need to carefully select optimal promoters for constitutive gene expression in specific lineages [44, 45]. Consequently, undifferentiated, pluripotent ICM cells may be more permissive than differentiated TE cells to the re-expression of EF1α, which drives the Tet-On 3G transactivator and/or the minimal CMV promoter, which forms part of the synthetic TRE3G promoter. Both CMV and TRE promoters show high cell type variability in expression strength, with the further complication that different

19

cell types respond differently to Dox dosage in terms of drug sensitivity and maximum expression level [46].

Concomitant with *Kdm4b* re-expression in the ICM, induced SCT embryos were significantly hypomethylated for H3K9/36me3 compared to non-induced controls, while the trend towards H3K9/36me3 hypomethylation was not significant in the TE. Induced SCT embryos also showed normal H3K9me3 levels that did not differ from IVF controls, while non-induced SCT embryos were hypermethylated in both ICM and TE.

Pig SCT embryos that were injected with porcine *KDM4A* mRNA showed significantly reduced levels at the 2-cell and blastocyst-stage [22]. This differs from our observations in 2-cells, which is likely due to the different time points of providing exogenous *Kdm4*. In our experiments, *Kdm4b* expression in the donor cells was quickly extinguished and did not prevent re-methylation of the somatic genome within 3-24 hours after SCT. In the pig mRNA injection experiments, *Kdm4* expression started at the earliest 5 hr post-activation, corresponding to at least 5 h after SCT, depending on the time interval between fusion and activation. Thus, H3K9me3 demethylation in pig began at a time point when H3K9me3 re-methylation was already complete in our experiments. As further discussed below, this delay in demethylation may be a conceptual advantage of mRNA injection over using hypomethylated donor cells.

In all these studies, H3K9me3 levels were assessed by IF, which provides a read-out of global methylation levels. It cannot be excluded that certain somatic reprogramming-resistant genomic regions remained hypomethylated [18, 19]. Continued activation of locally H3K9/36me3-depleted regions may persist for some time, making the genes in these regions worthwhile candidates for further investigation in *Kdm4b*-induced vs non-induced SCT embryos at EGA. Thus, even a short-lived decrease in H3K9/36me3 levels could facilitate initial binding of oocyte reprogramming factors, triggering a ripple effect that persists after the global differences in H3K9/36me3 have

20

disappeared. A similar effect was observed after knockdown of *Xist* in cloned male mouse morulae [13, 14]. Even though *Xist* expression returned to normal levels at the blastocyst stage, this transient *Xist* repression reactivated a number of X-linked genes in male cloned blastocysts and greatly improved their survival to term [13, 14].

Kmd4-dependent hypomethylation and totipotency reprogramming

The discussed gene expression and epigenetic changes underlie the significantly improved blastocyst formation rate observed in all mRNA *Kdm4*-overexpression studies to-date, be it in donor cells [15, 16, 23] or in embryos [17-22]. However, blastocyst formation is a poor indicator for developmental competence [34]. Instead, development into healthy adult animals is the most definitive measure of extensive donor cell reprogramming [34]. *Kdm4b* expression in donor cells did not improve production of live calves. This is in contrast to another cattle study, which found pregnancy, birth and survival rates to be significantly higher in both *KDM4D-* and *KDM4E*-injected SCT embryos [21]. The overall increase in cloning efficiency by *KDM4D-* or *KDM4E*-injection was about 6-fold, an effect that we would have been able to detect statistically with the numbers of embryos transferred in our experiments.

The main differences between both studies are i) the variants used (*i.e.* C-terminally truncated murine *Kdm4b* vs full-length bovine *KDM4D/E*) and ii) the method of *Kmd4* delivery (*i.e.* fusing multi-transgenic donor cells vs injecting mRNA into embryos). Truncated *Kdm4b* contained the JmjN domain, required for the activity of the JmjC catalytic center, but lacked the non-catalytic readers (Zn-finger PHD and double Tudor domains) that recognize specific histone lysine methylations [47]. These interactions target KDM4 to chromatin and regulate its activity, which is central to identify specific substrates and catalyse demethylation [47]. The KDM4B reader domains are also present in KDM4A and KDM4C [48]. They mediate exclusive binding to H3K23me3,

21

stimulating the demethylase activity of full-length KDM4B towards H3K36me3 [48]. Deleting

the C-terminal domain in KDM4 proteins can disrupt the cross-talk between reader and eraser

domains, changing sub-cellular localization and demethylase activity, via altered chromatin

affinity and/or protein complex formation with associated factors [49, 50]. However, we [15, 16]

and others [25] showed that the PHD and Tudor domains are dispensable for reducing

H3K9/36me3, but not H3K9me1/2 or H3K27me3, suggesting that truncated KDM4B would have

achieved appropriate functionality in embryos. Similar to truncated KDM4B, both the PHD and

Tudor domains are lacking in KDM4D/E. In contrast to full-length and truncated KDM4B,

however, KDM4D/E has a different substrate specificity: it does not demethylate H3K36me3, yet

attacks dimethylated in addition to trimethylated H1.4K26 [51, 52]. Furthermore, KDM4D

demethylates H3K9me2 with similar efficiency as H3K9me3 and may even demethylate

H3K9me1 [53, 54]. These differences may help to explain why KDM4D/E variants have improved

cloning efficiency in mouse [18], macaque [20] and cattle [21], while studies with truncated

KDM4B in mice [15] or injection of full-length *KDM4A* mRNA in pig [22] have not. In pig, it was

also noted that KDM4A mediated demethylation of the *XIST* promoter, resulting in *XIST*

derepression [22]. Even though significantly elevated *XIST* expression was not observed with

porcine KDM4B (or KDM4D), it would be important to investigate potential deregulation of *XIST*

in female *Kdm4b*-BEFs and SCT embryos. If a similar phenomenon occurred with *Kdm4b* in cattle,

this could have hindered long-term benefits in our experiments. In summary, it is plausible that

possessing H3K36me3 demethylase activity and/or lacking H3K9me1/2 and H1.4K26me3

demethylase activity interferes with long-term SCT-reprogramming success.

Different delivery approaches may have also contributed to the lack of a long-term beneficial effect in our experiments. Kdm4b-Egfp protein expression was no longer detectable within 8 hours after SCT and not re-induced by Dox at the 2-cell stage. It is likely that *Kdm4b*-expressing BEFs did not re-activate transgene transcription until EGA, which commences at the 8-cell stage in cattle [21], and has been widely accepted as a crucial milestone for restoring totipotency during normal development [55, 56]. At this stage, bovine IVF embryos were most susceptible to *KDM4E* silencing and increased H3K9me3 staining, indicating increased heterochromatin formation and gene silencing posing a developmental barrier. [21]. It is possible that by preferentially derepressing reprogramming-resistant regions, KDM4B prolongs a globally permissive chromatin state that is beneficial for totipotency reprogramming. Prolonging this relaxed chromatin state may delay establishment of repressive chromatin and activation of EGA-specific promoters and enhancers that ensure accurate control of embryonic transcription. Some of these H3K9me3-repressed regions include repeat elements, such as retrotransposons, that are also strongly up-regulated around EGA [55, 56]. In the absence of inducible *Kdm4b*-expression at EGA, none of these potential benefits would have been achieved. By contrast, bovine *KDM4D/E* mRNA injection post-activation significantly improved totipotency reprogramming [21]. Apart from using a different KDM4 variant, this approach may have been more beneficial as it does not require transcription in a non-permissive environment prior to EGA but instead only relies on translation of the injected mRNA at the 1-cell stage. To directly distinguish variant vs delivery effects, *Kdm4b and KDM4D/E* bovine donor cells and mRNA injection of the different variants will be included in future comparisons.

23

In summary, we demonstrate that targeted reduction of repressive H3K9/36me3 marks (via *Kdm4b* overexpression), potentiated by global histone hypomethlation (via serum starvation), led to a derestricted genome with greater *in vitro* reprogrammability. Sustained *Kdm4b* overexpression in serum-starved BEFs and BEF-derived embryos improved reprogramming into cloned embryos. However, neither this cell-based approach, nor the injection method [22] have so far consistently improved epigenetic reprogramming into totipotency, emphasizing that KDM4-assisted SCT methods require empirical optimisation of the KDM4 variant and delivery method before being generally applicable to the cloning of livestock species. The surviving cloned cow conditionally overexpresses KDM4B, providing a new transgenic animal model to study the remodeling of heterochromatin architecture during differentiation and assess alternative strategies for removing H3K9/36me3 marks during nuclear reprogramming of different somatic and embryonic cell types.

REFERENCES

1. Morgan HD, Santos F, Green K, Dean W, Reik W. Epigenetic reprogramming in mammals. Hum Mol Genet 2005; 14 Spec No 1:R47-58.
2. Yamanaka S, Blau HM. Nuclear reprogramming to a pluripotent state by three approaches. Nature 2010; 465:704-712.
3. Pasque V, Jullien J, Miyamoto K, Halley-Stott RP, Gurdon JB. Epigenetic factors influencing resistance to nuclear reprogramming. Trends Genet 2011; 27:516-525.
4. Kang YK, Park JS, Koo DB, Choi YH, Kim SU, Lee KK, Han YM. Limited demethylation leaves mosaic-type methylation states in cloned bovine pre-implantation embryos. Embo J 2002; 21:1092-1100.
5. Santos F, Zakhartchenko V, Stojkovic M, Peters A, Jenuwein T, Wolf E, Reik W, Dean W. Epigenetic marking correlates with developmental potential in cloned bovine preimplantation embryos. Curr Biol 2003; 13:1116-1121.
6. Fukuda A, Cao F, Morita S, Yamada K, Jincho Y, Tane S, Sotomaru Y, Kono T. Identification of inappropriately reprogrammed genes by large-scale transcriptome analysis of individual cloned mouse blastocysts. PLoS ONE 2010; 5:e11274.
7. Ogura A, Inoue K, Wakayama T. Recent advancements in cloning by somatic cell nuclear transfer. Philos Trans R Soc Lond B Biol Sci 2013; 368:20110329.
8. Kishigami S, Mizutani E, Ohta H, Hikichi T, Thuan NV, Wakayama S, Bui HT, Wakayama T. Significant improvement of mouse cloning technique by treatment with trichostatin A after somatic nuclear transfer. Biochem Biophys Res Commun 2006; 340:183-189.
9. Zhao J, Ross JW, Hao Y, Spate LD, Walters EM, Samuel MS, Rieke A, Murphy CN, Prather RS. Significant improvement in cloning efficiency of an inbred miniature pig by histone deacetylase inhibitor treatment after somatic cell nuclear transfer. Biol Reprod 2009; 81:525-530.
10. Sangalli JR, De Bem TH, Perecin F, Chiaratti MR, Oliveira Lde J, de Araujo RR, Valim Pimentel JR, Smith LC, Meirelles FV. Treatment of nuclear-donor cells or cloned zygotes with chromatin-modifying agents increases histone acetylation but does not improve full-term development of cloned cattle. Cell Reprogram 2012; 14:235-247.
11. Hosseini SM, Dufort I, Nieminen J, Moulavi F, Ghanaei HR, Hajian M, Jafarpour F, Forouzanfar M, Gourbai H, Shahverdi AH, Nasr-Esfahani MH, Sirard MA. Epigenetic modification with trichostatin A does not correct specific errors of somatic cell nuclear transfer at the transcriptomic level; highlighting the non-random nature of oocyte-mediated reprogramming errors. BMC Genomics 2016; 17:16.
12. Akagi S, Matsukawa K, Mizutani E, Fukunari K, Kaneda M, Watanabe S, Takahashi S. Treatment with a histone deacetylase inhibitor after nuclear transfer improves the preimplantation development of cloned bovine embryos. J Reprod Dev 2011; 57:120-126.
13. Inoue K, Kohda T, Sugimoto M, Sado T, Ogonuki N, Matoba S, Shiura H, Ikeda R, Mochida K, Fujii T, Sawai K, Otte AP, et al. Impeding Xist expression from the active X chromosome improves mouse somatic cell nuclear transfer. Science 2010; 330:496-499.
14. Matoba S, Inoue K, Kohda T, Sugimoto M, Mizutani E, Ogonuki N, Nakamura T, Abe K, Nakano T, Ishino F, Ogura A. RNAi-mediated knockdown of Xist can rescue the impaired postimplantation development of cloned mouse embryos. Proc Natl Acad Sci U S A 2011; 108:20621-20626.

15. Antony J, Oback F, Chamley LW, Oback B, Laible G. Transient JMJD2B-Mediated Reduction of H3K9me3 Levels Improves Reprogramming of Embryonic Stem Cells into Cloned Embryos. Mol Cell Biol 2013; 33:974-983.
16. Wei J, Antony J, Meng F, MacLean P, Rhind R, Laible G, Oback B. KDM4B-mediated reduction of H3K9me3 and H3K36me3 levels improves somatic cell reprogramming into pluripotency. Sci Rep 2017; 7:7514.
17. Liu W, Liu X, Wang C, Gao Y, Gao R, Kou X, Zhao Y, Li J, Wu Y, Xiu W, Wang S, Yin J, et al. Identification of key factors conquering developmental arrest of somatic cell cloned embryos by combining embryo biopsy and single-cell sequencing. Cell Discovery 2016; 2:16010.
18. Matoba S, Liu Y, Lu F, Iwabuchi KA, Shen L, Inoue A, Zhang Y. Embryonic development following somatic cell nuclear transfer impeded by persisting histone methylation. Cell 2014; 159:884-895.
19. Chung YG, Matoba S, Liu Y, Eum JH, Lu F, Jiang W, Lee JE, Sepilian V, Cha KY, Lee DR, Zhang Y. Histone Demethylase Expression Enhances Human Somatic Cell Nuclear Transfer Efficiency and Promotes Derivation of Pluripotent Stem Cells. Cell Stem Cell 2015; 17:758-766.
20. Liu Z, Cai Y, Wang Y, Nie Y, Zhang C, Xu Y, Zhang X, Lu Y, Wang Z, Poo M, Sun Q. Cloning of Macaque Monkeys by Somatic Cell Nuclear Transfer. Cell 2018; 172:881-887.e887.
21. Liu X, Wang Y, Gao Y, Su J, Zhang J, Xing X, Zhou C, Yao K, An Q, Zhang Y. H3K9 demethylase KDM4E is an epigenetic regulator for bovine embryonic development and a defective factor for nuclear reprogramming. Development 2018; 145.
22. Ruan D, Peng J, Wang X, Ouyang Z, Zou Q, Yang Y, Chen F, Ge W, Wu H, Liu Z, Zhao Y, Zhao B, et al. XIST Derepression in Active X Chromosome Hinders Pig Somatic Cell Nuclear Transfer. Stem Cell Reports 2018; 10:494-508.
23. Zhang Y, Wang Q, Liu K, Gao E, Guan H, Hou J. Treatment of donor cells with recombinant KDM4D protein improves preimplantation development of cloned ovine embryos. Cytotechnology 2018.
24. Kallingappa PK, Turner PM, Eichenlaub MP, Green AL, Oback FC, Chibnall AM, Wells DN, Oback B. Quiescence Loosens Epigenetic Constraints in Bovine Somatic Cells and Improves Their Reprogramming into Totipotency. Biol Reprod 2016; 95:1-10.
25. Fodor BD, Kubicek S, Yonezawa M, O'Sullivan RJ, Sengupta R, Perez-Burgos L, Opravil S, Mechtler K, Schotta G, Jenuwein T. Jmjd2b antagonizes H3K9 trimethylation at pericentric heterochromatin in mammalian cells. Genes Dev 2006; 20:1557-1562.
26. Woltjen K, Michael IP, Mohseni P, Desai R, Mileikovsky M, Hamalainen R, Cowling R, Wang W, Liu P, Gertsenstein M, Kaji K, Sung HK, et al. piggyBac transposition reprograms fibroblasts to induced pluripotent stem cells. Nature 2009; 458:766-770.
27. Loew R, Heinz N, Hampf M, Bujard H, Gossen M. Improved Tet-responsive promoters with minimized background expression. BMC Biotechnol 2010; 10:81.
28. Wang W, Lin C, Lu D, Ning Z, Cox T, Melvin D, Wang X, Bradley A, Liu P. Chromosomal transposition of PiggyBac in mouse embryonic stem cells. Proc Natl Acad Sci U S A 2008; 105:9290-9295.
29. Wells DN, Laible G, Tucker FC, Miller AL, Oliver JE, Xiang T, Forsyth JT, Berg MC, Cockrem K, L'Huillier PJ, Tervit HR, Oback B. Coordination between donor cell type and cell cycle stage improves nuclear cloning efficiency in cattle. Theriogenology 2003; 59:45-59.

30. Meng F, Forrester-Gauntlett B, Turner P, Henderson H, Oback B. Signal Inhibition Reveals JAK/STAT3 Pathway as Critical for Bovine Inner Cell Mass Development. Biol Reprod 2015; 93:132.

31. Oback B, Wells DN. Cloning cattle. Cloning Stem Cells 2003; 5:243-256.

32. Schurmann A, Wells DN, Oback B. Early zygotes are suitable recipients for bovine somatic nuclear transfer and result in cloned offspring. Reproduction 2006; 132:839-848.

33. Payen E, Verkerk T, Michalovich D, Dreyer SD, Winterpacht A, Lee B, De Zeeuw CI, Grosveld F, Galjart N. The centromeric/nucleolar chromatin protein ZFP-37 may function to specify neuronal nuclear domains. J Biol Chem 1998; 273:9099-9109.

34. Oback B, Wells DN. Donor cell differentiation, reprogramming, and cloning efficiency: elusive or illusive correlation? Mol Reprod Dev 2007; 74:646-654.

35. Canzio D, Liao M, Naber N, Pate E, Larson A, Wu S, Marina DB, Garcia JF, Madhani HD, Cooke R, Schuck P, Cheng Y, et al. A conformational switch in HP1 releases auto-inhibition to drive heterochromatin assembly. Nature 2013; 496:377-381.

36. Poleshko A, Katz RA. Specifying peripheral heterochromatin during nuclear lamina reassembly. Nucleus 2014; 5:32-39.

37. Zhang T, Cooper S, Brockdorff N. The interplay of histone modifications - writers that read. EMBO Rep 2015; 16:1467-1481.

38. Ohhata T, Matsumoto M, Leeb M, Shibata S, Sakai S, Kitagawa K, Niida H, Kitagawa M, Wutz A. Histone H3 Lysine 36 Trimethylation Is Established over the Xist Promoter by Antisense Tsix Transcription and Contributes to Repressing Xist Expression. Mol Cell Biol 2015; 35:3909-3920.

39. Oikawa M, Matoba S, Inoue K, Kamimura S, Hirose M, Ogonuki N, Shiura H, Sugimoto M, Abe K, Ishino F, Ogura A. RNAi-mediated knockdown of Xist does not rescue the impaired development of female cloned mouse embryos. J Reprod Dev 2013; 59:231-237.

40. Probst AV, Okamoto I, Casanova M, El Marjou F, Le Baccon P, Almouzni G. A strand-specific burst in transcription of pericentric satellites is required for chromocenter formation and early mouse development. Dev Cell 2010; 19:625-638.

41. Kigami D, Minami N, Takayama H, Imai H. MuERV-L is one of the earliest transcribed genes in mouse one-cell embryos. Biol Reprod 2003; 68:651-654.

42. Liu H, Kim J-M, Aoki F. Regulation of histone H3 lysine 9 methylation in oocytes and early pre-implantation embryos. Development 2004; 131:2269-2280.

43. Chen C-m, Krohn J, Bhattacharya S, Davies B. A Comparison of Exogenous Promoter Activity at the ROSA26 Locus Using a PhiC31 Integrase Mediated Cassette Exchange Approach in Mouse ES Cells. PLOS ONE 2011; 6:e23376.

44. Norrman K, Fischer Y, Bonnamy B, Wolfhagen Sand F, Ravassard P, Semb H. Quantitative Comparison of Constitutive Promoters in Human ES cells. PLOS ONE 2010; 5:e12413.

45. Bagchi B, Kumar M, Mani S. CMV promotor activity during ES cell differentiation: potential insight into embryonic stem cell differentiation. Cell biology international 2006; 30:505-513.

46. Qin JY, Zhang L, Clift KL, Hulur I, Xiang AP, Ren B-Z, Lahn BT. Systematic Comparison of Constitutive Promoters and the Doxycycline-Inducible Promoter. PLOS ONE 2010; 5:e10611.

47. Dimitrova E, Turberfield AH, Klose RJ. Histone demethylases in chromatin biology and beyond. EMBO Rep 2015; 16:1620-1639.

48. Su Z, Wang F, Lee J-H, Stephens KE, Papazyan R, Voronina E, Krautkramer KA, Raman A, Thorpe JJ, Boersma MD, Kuznetsov VI, Miller MD, et al. Reader domain specificity and lysine demethylase-4 family function. Nature Communications 2016; 7:13387.

49. Lohse B, Helgstrand C, Kristensen JBL, Leurs U, Cloos PAC, Kristensen JL, Clausen RP. Posttranslational Modifications of the Histone 3 Tail and Their Impact on the Activity of Histone Lysine Demethylases In Vitro. PLOS ONE 2013; 8:e67653.

50. Kupershmit I, Khoury-Haddad H, Awwad SW, Guttmann-Raviv N, Ayoub N. KDM4C (GASC1) lysine demethylase is associated with mitotic chromatin and regulates chromosome segregation during mitosis. Nucleic Acids Research 2014; 42:6168-6182.

51. Krishnan S, Trievel RC. Structural and functional analysis of JMJD2D reveals molecular basis for site-specific demethylation among JMJD2 demethylases. Structure 2013; 21:98-108.

52. Trojer P, Zhang J, Yonezawa M, Schmidt A, Zheng H, Jenuwein T, Reinberg D. Dynamic Histone H1 Isotype 4 Methylation and Demethylation by Histone Lysine Methyltransferase G9a/KMT1C and the Jumonji Domain-containing JMJD2/KDM4 Proteins. J Biol Chem 2009; 284:8395-8405.

53. Hillringhaus L, Yue WW, Rose NR, Ng SS, Gileadi C, Loenarz C, Bello SH, Bray JE, Schofield CJ, Oppermann U. Structural and evolutionary basis for the dual substrate selectivity of human KDM4 histone demethylase family. J Biol Chem 2011; 286:41616-41625.

54. Couture JF, Collazo E, Ortiz-Tello PA, Brunzelle JS, Trievel RC. Specificity and mechanism of JMJD2A, a trimethyllysine-specific histone demethylase. Nat Struct Mol Biol 2007; 14:689-695.

55. Zhou LQ, Dean J. Reprogramming the genome to totipotency in mouse embryos. Trends Cell Biol 2015; 25:82-91.

56. Ishiuchi T, Torres-Padilla ME. Towards an understanding of the regulatory mechanisms of totipotency. Curr Opin Genet Dev 2013; 23:512-518.

28

FIGURE LEGENDS

Figure 1. Dox-inducible *Kdm4b-Egfp* expression in rejuvenated bovine fibroblasts (A) The

piggyBac (PB) transposon vector used to deliver expression of tetracycline-responsive (TRE3G),

puromycin-linked (IRES-puro-pA) histone demethylase (*Kdm4b-Egfp*). 3′/5′TR=pB terminal

repeats; **(B)** Strategy for using somatic cell transfer (SCT) cloning to rejuvenate stable Dox-

inducible BEFs that overexpress *Kdm4b-Egfp*. **(C)** Flow cytometry analyses of KDM4B-EGFP

induction in rejuvenated clonal BEF strains #1 (left) and #2 (right). Green fluorescence was

determined using the FL1 EGFP emission channel. The range of intensities for green fluorescent

cells (P2) is indicated. Relative cell number counts are plotted as a function of variable intensities of

green fluorescence from individual cells. Line graph: non-induced (black line) vs induced (green

line) cells; red line: induced cells one day after Dox-removal.

29

A.

3'TR — P_{TRE3G} — *Kdm4b-Egfp* — IRES — *Puro^r* — pA — 5'TR

B.

$P_{EF-1\alpha}$ — *Tet-On 3G* — P_{SV40} — *Neo^r*

BEF5 → 1. Rejuvenate by SCT cloning → BEF5_Tet

P_{TRE3G} — *Kdm4b-Egfp* — IRES — *Puro^r*

→ 2. Rejuvenate by SCT cloning → BEF5_Tet_KDM4B-EGFP

C.

-DOX
+DOX (24h)
+DOX (24h), -DOX (24h)

P2 85%

EGFP (clone #1)

-DOX
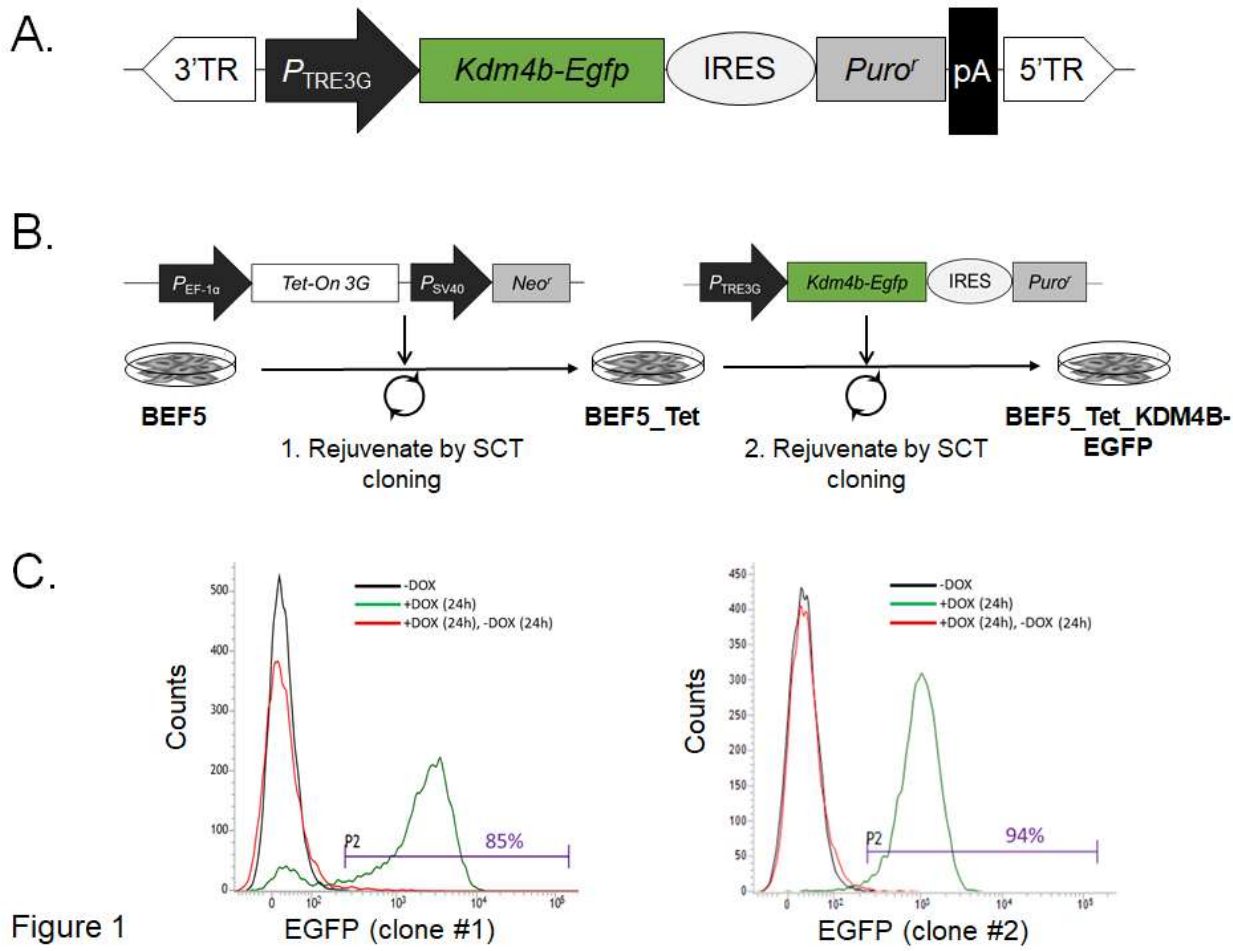+DOX (24h)
+DOX (24h), -DOX (24h)

P2 94%

EGFP (clone #2)

Figure 1

30

Figure 2. *Kdm4b*-dependant changes of histone trimethylation levels in BEFs (A)

Immunofluorescence analyses of different H3Kme3 modifications in non-induced (NI) and induced

(I) *Kdm4b*-BEFs that were either serum-starved or non-starved. Cells were co-stained for DNA and

with antibodies specific for EGFP and the indicated histone modification. Arrowheads and arrows

indicate EGFP-positive and –negative nuclei, respectively, within the induced population. **(B)**

Quantification of global H3Kme3 levels of indicated histone modifications from

immunofluorescence images. Values represent normalized pixel intensity (region of interest/area) ±

SEM. Asterisks indicate significant differences. N=number of nuclei quantified, n=3 biological

replicates, RU=relative units; ***P<0.001; as determined by 2–tailed t-test. **(C)** Western analyses of

histone extracts from induced (I) and non-induced (NI) *Kdm4b*-BEFs. Shown are representative

immunoblots for three different methyl states of H3, normalized on three prominent invariant bands

in the Ponceau stain. **(D)** Quantification of western analysis. Values represent normalized band

intensity (histone modification/Ponceau) ± SEM determined from 3 biological repeats; RU=relative

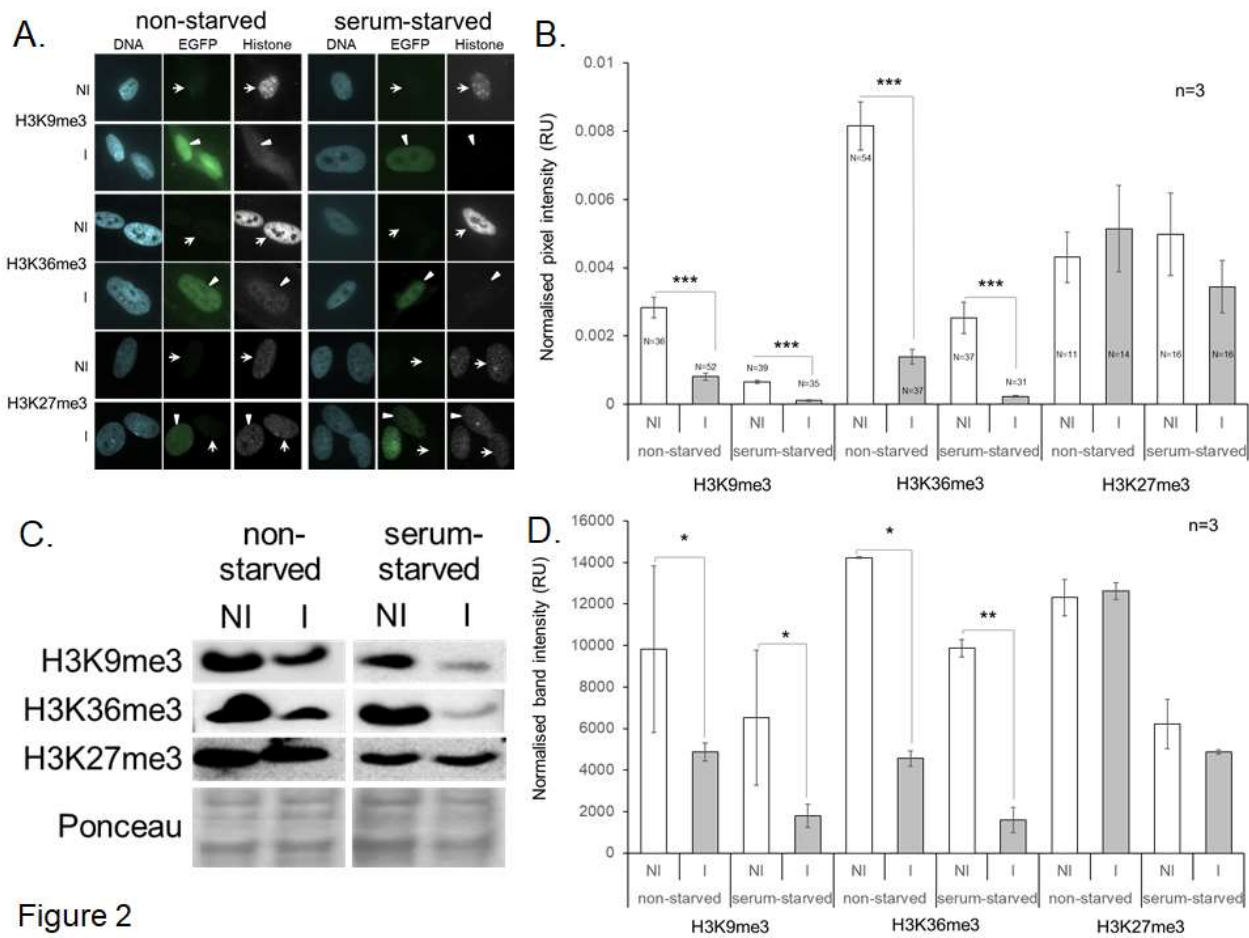units; *, **: P<0.05 and P<0.01, respectively, as determined by 2–tailed t-test.

31

Figure 2

Figure 3. *Kdm4b*-dependant upregulation of *ZFP37* in serum-starved, induced BEFs. Shown are the relative expression levels of transgene-derived *Kdm4b* and *ZFP37*, relative to 18S expression (n=3 biological replicates), as measured by RT-qPCR. Results for non-induced (NI) and induced (I) *Kdm4b*-BEFs are represented by grey and white bars ± SEM, respectively, *=P<0.05.
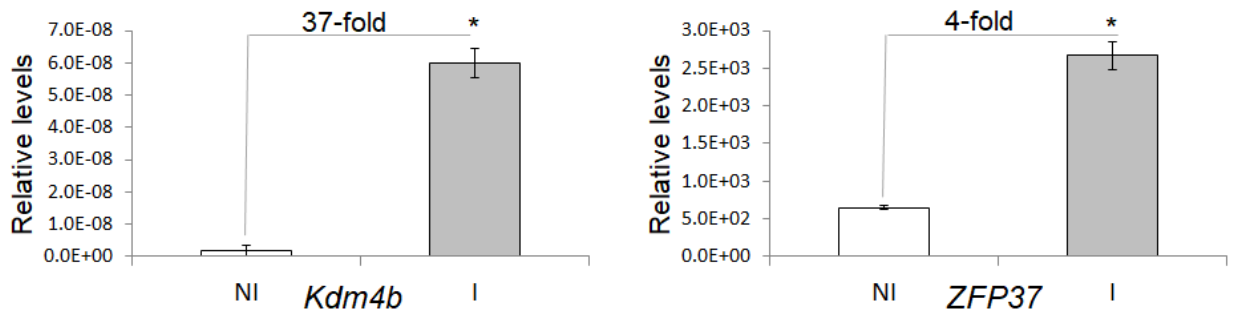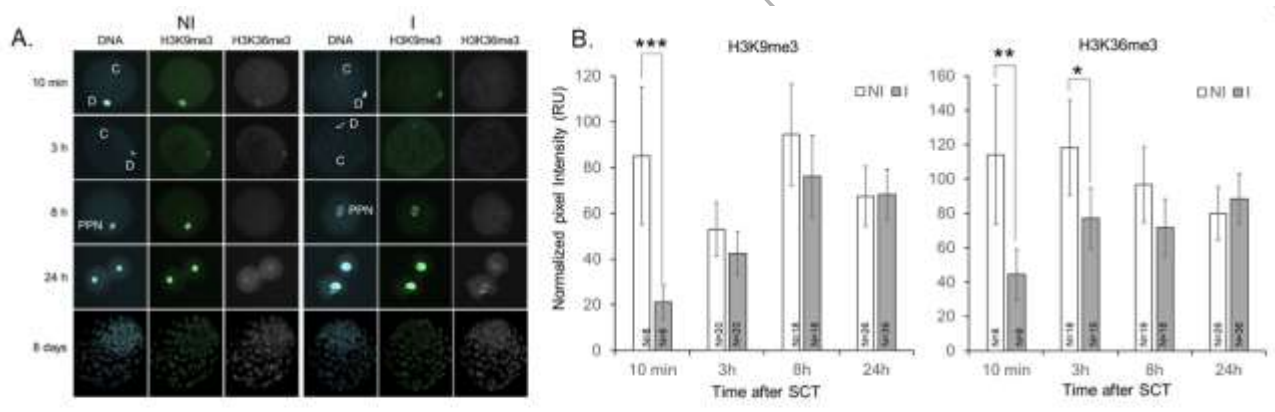

Figure 3

Figure 4. Characterization of global H3K9me3 and H3K36me3 levels following SCT with

Kdm4b-**BEFs.** SCT reconstructs were fixed and stained with H33342 (DNA) and antibodies

specific for H3K9me3 and H3K36me3. **(A)** Dox-induced (I) and non-induced (NI) SCT

reconstructs were analysed 10 minutes (upper panel), 3 h, 8 h, 24 h and 8 days (lower panel) after

fusion of the donor cell with an enucleated oocyte (cytoplast). C= cytoplast; D=donor DNA;

PPN=pseudo-pronucleus. **(B)** Quantification of immunofluorescence analysis in (A). Values

represent normalized pixel intensity (region of interest/area) ± SEM in relative units (RU).

N=number of SCT reconstructs analysed. Asterisks indicate significant differences between BEFs

from the same groups (induced or non-induced) at different time points, ***P<0.0001, **P<0.01,

*P≤0.05 as determined by 2–tailed t-test.

Revised Figure 4

34

Table 1. *In vitro* development of SCT embryos from induced vs non-induced *Kdm4b*-BEF donor

cells

Donor treatment	Embryo treatment	n	N	No. of ≥1-cells (% ± SEM)	No. of B1-3 (% ± SEM)[†]
NI	NI	4	133	101 (76 ± 5%)	69 (52 ± 2%)
I	NI	4	152	118 (78 ± 4%)	76 (50 ± 3%)

Embryos were cloned from serum-starved donor cells (clonal strain #1) exposed to Dox (I) or buffer

(NI) and cultured in medium without Dox (NI); n = number of independent SCT experiments;

[†]percentage of embryos placed into IVC (N) that developed into D8 blastocysts (B) grade 1-3 (B^{1-3})

or into B grade 1-2 (B^{1-2})

Table 2. *In vitro* development of induced vs non-induced SCT embryos

Donor treatment	Embryo treatment	n	N	No. of ≥1-cells (% ± SEM)	No. of B1-3 (% ± SEM)[†]
NI	NI	8	440	420 (96 ± 1%)	177 (40 ± 0.3%)***
I	I	8	462	462 (96 ± 1%)	256 (55 ± 0.2%)

Embryos were cloned from serum-starved donor cells (clonal strains #1 and #2) exposed to Dox (I)

or buffer (NI) and cultured in medium containing Dox (I) or buffer (NI). n = number of independent

NT experiments; [†]percentage of embryos placed into IVC (N) that developed into D8 blastocysts

(B) grade 1-3 (B^{1-3}) or into B grade 1-2 (B^{1-2}); ***,* rows within a column differ *P*<0.0001 and

P<0.01, respectively. Significance was determined via Fisher 2x2 test.

Table 3. *In vivo* development of induced vs non-induced SCT embryos

Donor group	Embryo group	n	N	D35 (% ± SEM) †	D60 (% ± SEM) †	D90 (% ± SEM) †	D120 (% ± SEM) †	D150 (% ± SEM) †	D180 (% ± SEM) †	D210 (% ± SEM) †	Term (% ± SEM) †	Adult (% ± SEM) †
NI	NI	3	32	12 (38 ± 6%)	11 (34 ± 8%)	4 (13 ± 8%)	4 (13 ± 8%)	3 (9 ± 8%)	2 (6 ± 7%)	2 (6 ± 4%)	1 (3 ± 2%)	1 (3 ± 2%)
I	I	3	33	13 (39 ± 1%)	8 (24 ± 10%)#	3 (9 ± 7%)	2 (6 ± 4%)	2 (6 ± 4%)	0	0	0	0

Embryos were cloned from serum-starved donor cells (clonal strains #1 and #2) exposed to Dox (I) or buffer (NI) and cultured in medium containing Dox (I) or buffer (NI). n = number of independent SCT experiments; †percentage of D8 blastocysts (N) that developed to this stage. #Two viable fetuses from the induced group were removed for cell line rejuvenation on D42 and D57, respectively, and numbers reduced accordingly. Potential survival of these fetuses would not have introduced significant differences between the two treatment groups.